The 9th European Congress on Computational Methods in Applied Sciences and Engineering
ECCOMAS Congress 2024
3–7 June 2024, Lisboa, Portugal

FLOW CONTROL WITH DATA DRIVEN APPROACHES FOR LAMINAR FLAMES

ADRIÁN CORROCHANO[1,*], JUAN LUIS CANALS[1], LAURA SAAVEDRA[1] AND SOLEDAD LE CLAINCHE[1,2]

[1] ETSI Aeronáutica y del Espacio, Universidad Politécnica de Madrid, Madrid, Spain

[*] Corresponding author: adrian.corrochanoc@upm.es

Key words: Computational Fluid Dynamics, Reacting Flows, Flow control

Summary. This article introduces a novel method to identify structural sensitivity, applied for the first time, to the authors' knowledge, in reactive flows. The method, so-called, non-linear structural sensitivity, identify the regions more sensible to the flow to structural changes. The method is applied to optimize the efficiency of a laminar pulsating flame, where the NO_x emissions are also controlled. The method is based on higher order dynamic mode decomposition (HODMD), therefore it is fully data-driven and generalizable for different conditions of the flow and different geometries. The results presented show great potential for the algorithm to be used in flow control applications and the design of components for pollutant reduction.

1 INTRODUCTION

Optimization and flow control in fluid dynamics is a research topic of high interest because of its multiple industrial applications, ranging from the design of aircrafts and space vehicles to microfluidic devices [1]. An optimal design of such devices can reduce the drag or the noise and increase the efficiency of those industrial devices. Modelling complex flows is a challenging problem due to the need of large computational resources and the complexity of the underlying physical problem [2]. In terms of combustion control, in addition to these mentioned problems, the large number of species involved in combustion processes, the range of scales, and the turbulence-chemistry interaction require large computational resources [3].

Flow control encompasses active and passive flow control. Active flow control is the one which involves external energy or active mechanisms to influence the flow. On the other hand, passive flow control does not introduce any source of energy. These techniques can be achieved through the design of the industrial devices, adding objects or modifying the shape. In his work, passive flow control for reactive flows is pursued to increase the efficiency of the flame and reduce the emission of pollutants, without adding any external source of energy. In this sense, not many studies have been carried out. Karagozian [4] explored the concept of the lobed fuel injector, which enhanced the local mixing and lowering the NO_x (nitrogen oxide) emissions with the change in the shape of the injector. Other examples included the addition of atomizers in combustion chambers [5] or transverse fuel injection into supersonic airflow [6]. What these techniques have in common is the fact that there is not a guideline of the location where to apply the passive flow control.

In non-reactive flows, it is possible to calculate the *structural sensitivity* [7]. This concept identifies the regions of the flow most sensitive to changes, therefore it has applications for flow control. To calculate the structural sensitivity, it is necessary to combine direct and adjoint solutions, what in realistic problems would be expensive in terms of computational memory and time. Recently, some approaches in the field of flow control have been carried out using data-driven methods, which would mean a substantial decrease in the cost. Deep reinforcement learning (DRL) has been used for active flow control in the flow past a cylinder [8] or in turbulent channel flows [9], both for drag reduction.

The present study extends our previous work [10], where we combine the knowledge about structural sensitivity with the use of fully data driven algorithms. The method has demonstrate to provide accurate results in laminar non reactive flows. The objective of the present work is to adapt this algorithm for laminar flames to increase the efficiency in the combustion and reduce the release of pollutants.

The article is organized as follows. Section 2 introduces the flow control algorithm. The numerical setup for the CFD simulation is shown and discussed in Section 3. Finally the main results and conclusions are presented in Sections 4 and 5, respectively.

2 METHODOLOGY

The proposed algorithm for passive flow control is based on Higher Order Dynamic Mode Decomposition (HODMD) [11]. HODMD is a data-driven algorithm that needs as an input datasets in matrix form. A group of K snapshots $\mathbf{v}_k$ equidistant in time is collected. Each snapshot is composed by $J = N_v \times N_x \times N_y$ points, where N_v is the number of variables and N_x and N_y are the grid points in the streamwise and normal directions, assuming a bidimensional structured grid. Therefore, the snapshot matrix $\mathbf{V}_1^K$ of dimensions $J \times K$ can be organised as follows

$$\mathbf{V}_1^K = [\mathbf{v}_1, \mathbf{v}_2, \ldots, \mathbf{v}_k, \mathbf{v}_{k+1}, \ldots, \mathbf{v}_{K-1}, \mathbf{v}_K], \tag{1}$$

HODMD [11] is an extension of dynamic mode decomposition (DMD) [12] used for the analysis of complex flows, showing potential in the study of various types of flows; such as non-newtonian turbulent flows [13] or reacting flows [14] and is also capable to identify global instabilities triggering changes in the flow [15, 16]. The algorithm decomposes spatio-temporal data $\mathbf{v}_k$ into a Fourier-like expansion of M DMD modes $\mathbf{u}_m$ as

$$\mathbf{v}(x, y, z, t_k) \simeq \sum_{m=1}^{M} a_m \mathbf{u}_m(x, y, z) e^{(\delta_m + i\omega_m)t_k}, \tag{2}$$

for $k = 1, \ldots, K$, where a_m is the amplitude, ω_m is the frequency and δ_m corresponds to the growth rate of the mode $\mathbf{u}_m$.

A more detailed description and applications of this algorithm can be found in [17], including the implementation of this algorithm in Matlab. More recently a version of the algorithm has been implemented in Python by [18].

Considering HODMD as the basis of the passive flow control algorithm, the method for calculating the so-called non-linear structural sensitivity can be summarised in four main steps:

Step 1: filtering the dynamics of the snapshot matrix. At this step, HODMD is applied to the snapshot matrix $\mathbf{V}_1^K$ to calculate the HODMD expansion (Eq. 2). The HODMD expansion will only retain the three highest amplitude modes: the mean flow (mode with $\omega = 0$ and the leading frequency mode with its complex conjugate. In this way, the dynamics of the complex flow are simplified and the noise is reduced. With the HODMD expansion, a filtered snapshot matrix $\widetilde{\mathbf{V}}_1^K$ is obtained. The leading frequency mode contains information about the main flow dynamics. The structural sensitivity will approximate the parts of the domain where it is possible to produce the strongest changes in the flow, controlling the shape and even the presence of this mode.

Step 2: Direct HODMD. HODMD is applied to the filtered snapshot matrix $\widetilde{\mathbf{V}}_1^K$, obtaining the *direct* HODMD expansion.

Step 3: Adjoint HODMD. To simplify the computation, the mean is substracted to the adjoint snapshot matrix, defined as $\widetilde{\mathbf{V}}_1^{K*} = \widetilde{\mathbf{V}}_K^1$, before applying the HODMD method. The mean is the same in both cases, the direct and the adjoint matrices.

Step 4: non-linear structural sensitivity. The structural sensitivity, called as *non-linear structural sensitivity* is calculated as

$$\tilde{\mathbf{S}}^{NL} = \omega||\mathbf{M}|| \cdot ||\mathbf{M}|| + 2||\mathbf{N}|| \cdot ||\mathbf{N}^*||, \tag{3}$$

where $\mathbf{M} = \bar{v}_j \frac{\partial \bar{v}_i}{\partial x_j}$, being $\bar{\mathbf{v}} = (\bar{v}_i, \bar{v}_j)$ the mean flow (HODMD mode with $\omega = 0$) of the direct solution and $\mathbf{x} = (x_i, x_j)$ the spatial dimensions. The term $\mathbf{N} = v'_j \frac{\partial v'_i}{\partial x_j}$, being $\mathbf{v}' = (v'_i, v'_j)$, is the direct mode with frequency ω and lastly, $\mathbf{N}^* = v^*_j \frac{\partial v^*_i}{\partial x_j}$, where $\mathbf{v}^* = (v^*_i, v^*_j)$, is the adjoint mode with frequency ω. The HODMD modes are weighted with their corresponding amplitudes, and normalized with their maximum value.

More details about the implementation of this algorithm for passive flow control can be found in [10], as well as different applications in fluid dynamics, comparing the results with classical linear methods.

3 SIMULATION SETUP

The studied case is the oxidation of a nitrogen-diluted methane jet. CFD simulations have been carried out for this laminar flame. The oxidizer is regular air injected into the domain at constant velocity of $35cm/s$, while the fuel, composed by 65% of methane and 35% of nitrogen, is injected according to the following sinusoidal parabolic velocity profile:

$$v(r,t) = v_{max}\left(1 - \frac{r^2}{R^2}\right)[1 + A\ sin(2\pi f\ t)], \tag{4}$$

where v_{max} is the maximum velocity ($v_{max} = 75cm/s$), r is the radial coordinate, R is the internal radius of the nozzle ($R = 2mm$), A is the amplitude of the sinusoidal perturbation ($A = 0.25$) and f is the frequency of the perturbation ($f = 10Hz$). The detailed kinetic mechanism used for the numerical simulation is `GRI-Mech 3.0` [19], taking into account 325 chemical reactions and 53 species, including the formation of oxides of nitrogen NO_x. The CFD

simulations were carried out using the solver *reactingFoam*, an OpenFOAM solver that accounts for transient, non-premixed combustion problems. A representative snapshot of the temperature is shown in Fig. 1. The results of the numerical simulation have been validated with previous studies [20, 21].

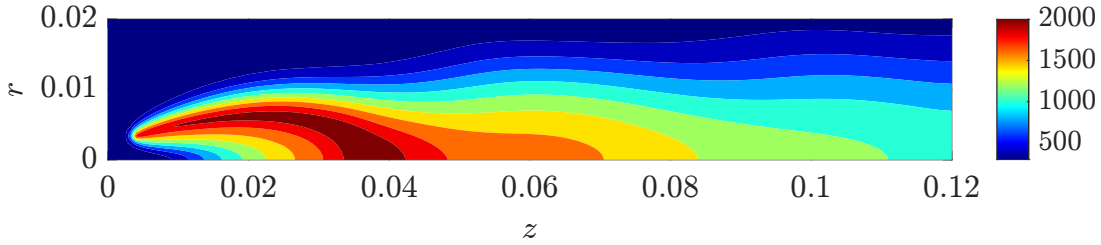

Figure 1: Instantaneous image of the temperature field of the numerical simulation analysed.

4 RESULTS

In this section, the flow control algorithm is applied to the simulation explained above. For that purpose, a database is extracted, consisting of snapshots with 19 variables (velocity field, temperature, pressure and 15 chemical species) and two spatial dimensions composed by a 150×150 grid points along the axial and radial directions. The snapshots are extracted each $\Delta t = 0.001s$ equidistant in time and a total of 1000 snapshots are extracted. Therefore the database is a fourth order tensor of dimensions $19 \times 150 \times 150 \times 1000$.

4.1 Application of HODMD and the non-linear strucutral sensitivity

The order of magnitude of the variables ranges from 10^5 (pressure field) to 10^{-6} (N_2O concentration), therefore the database needs to be pre-processed. The variables were centered to focus on the temporal perturbations and scaled with the range of each variable, as

$$\tilde{s}_j = \frac{s_j - \bar{s}_j}{max(s_j) - min(s_j)}, \tag{5}$$

where s_j is the j-th variable, $\bar{s}_j$ is its temporal mean, $max(s_j)$ and $min(s_j)$ are the maximum and minimum value; and $\tilde{s}_j$ is the pre-processed variable, following the advice proposed in [22, 14].

The application of HODMD to the preprocessed database can be found in Fig. 2. As it can be seen the spectrum is clearly periodic, with a frequency of $\omega \sim 63$. The frequency, as expected is equal as the one induced in the boundary condition of the fuel ($f = \omega/2\pi = 10Hz$). For the analysis of the modes, just the velocity is shown, although the analysis has been done to the 19 variables at the same time, and similar analysis can be carried out. The HODMD mode presents some coherent structures along the center line ($r = 0$), showing the movement of the reacting flow downstream.

From Eq.3, the non-linear structural sensitivity can be calculated. For the present work, both terms are going to be taken into account separately, to observe the structures provoked by the mode with 0 frequency and the mode with frequency ω. In this case, for the first term, the temporal mean of the simulation is used, as it has been removed from the database during the

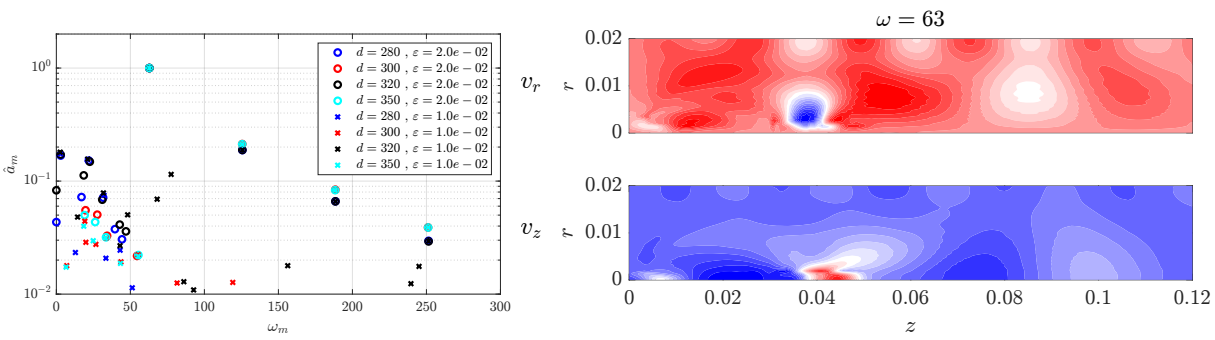

Figure 2: **Left:** Frequencies vs. Amplitudes corresponding to the HODMD modes of the studied database. **Right:** Real part of the leading mode for the velocity field, being v_r and v_z the radial and axial component, respectively. The mode has been normalized between values -1 and 1.

pre-processing. For the calculation of the sensitivity, just the velocity field is taken into account, however as the system is coupled, changes in the velocity should change the other variables.

In Fig. 3, the contours of the two terms are plotted. From the first term, the region with highest structural sensitivity appears between the two jets, while on the term related to the non-stationary mode two regions appear: one in the near field, close to the injection of fuel, and the other one, in the area where the HODMD mode has its highest amplitude. Based on these results, we study the changes produced in the flow in three different test cases, inserting a small circular cylinder (a punctual force is also valid) in the areas with the highest structural sensitivity. The position at which this cylinder is located in these three cases are the following:

1. **Case 1:** $x = 0.005$; $z = 0.004$
2. **Case 2:** $x = 0.001$; $z = 0.005$
3. **Case 3:** $x = 0.001$; $z = 0.037$

The location of the cylinders can be found in the bottom part of Fig. 3. The diameter of the cylinders is $0.0038m$, the same as the thickness of the wall separating the two jets. Other diameters can be chosen following the different characteristic length scales from the case under study (i.e., based on the temperature field, the diameter of the inner jet or the diameter of the outer jet). However this topic will remain open for future studies.

4.2 Analysis of the controlled cases

In this section, the three cases with a little cylinder are analysed. The efficiency and quality indicators are chosen attending to the different applications of the studied case. In particular, we analyse the temporal mean combustion efficiency and the concentration of NOx at the outlet. The efficiency is calculated as follows

$$\eta = \frac{1}{T}\int_0^T \left(1 - \frac{\dot{m}_{CO}Q_{CO} + \dot{m}_{H_2}Q_{H_2} + \dot{m}_{HC}Q_{HC}}{cL}\right) dt, \; HC = CH_4, C_2H_2, C_2H_4, C_2H_6, \quad (6)$$

where T is the final time, $\dot{m}_i = Y_i\dot{m}_{out}$ and Q_i are the outlet mass flux and the lower heating value of species i, respectively, $c = Y_{CH_4}\dot{m}_{in}$ is the fuel mass flux at the inlet and L is the lower

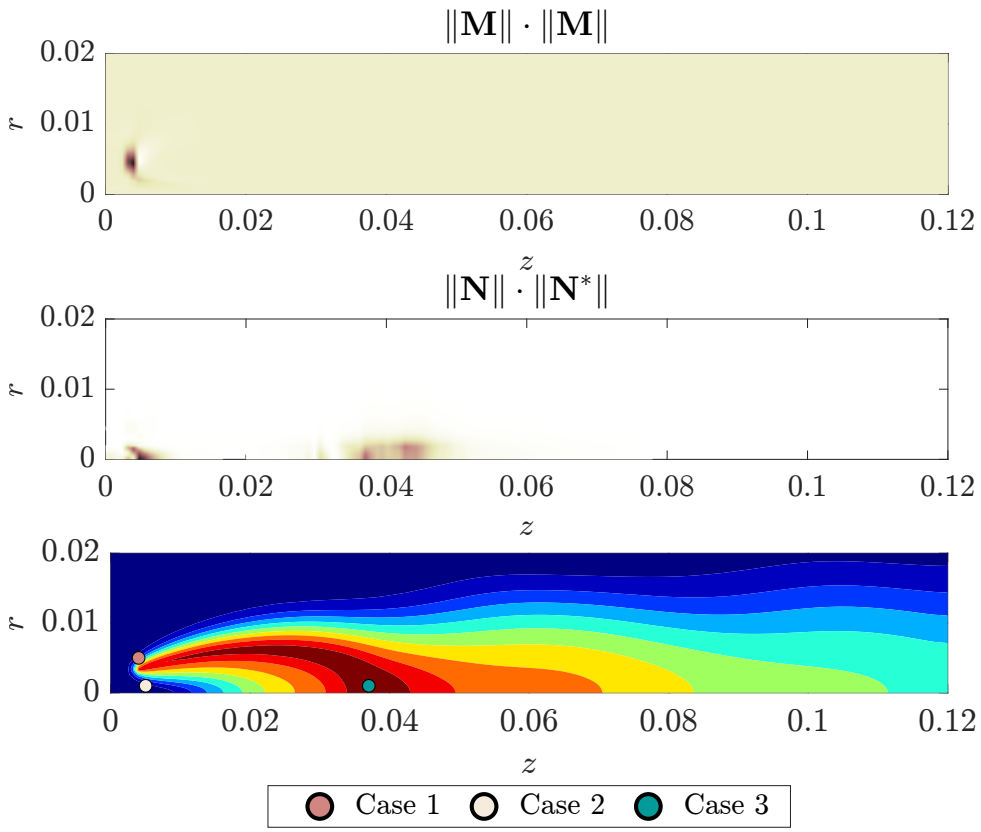

Figure 3: **From top to bottom:** Contour of the first term of the non-linear structural sensitivity, contour of the second term of the non-linear structural sensitivity and localization of the three cylinders over a representative snapshots of the temperature (the cylinders are bigger than in the simulations for a better visualization).

heating value of methane. This equation expresses how far is the full conversion of the fuel to the main products, which are H_2O and CO_2. Unburnt fuel or products will decrease the efficiency.

In Tab. 1 the vales of efficiency and NOx production are presented. Apart from the total NO_x production, also the two main components of NO_x are presented, i.e. NO and NO_2. The first case does not provide any optimum value, however, the NO_x production is lowered, in the total sum and in each component. The third case lowers the efficiency, however it decreases the NO production at the expense of increasing the NO_2 production. Lastly, the second case is best for overall combustion efficiency, including global NO_x emissions.

For understanding the dynamics of each case and the possible explanation of this increase in the efficiency or decrease in the NO_x emissions, the three cases are analized with HODMD. The spectrum in the three cases is periodic with the main frequency the same as the initial case $\omega = 63$. This is trivial, as the flow is forced in the boundary condition with that frequency, therefore the frequency and the mode related are going to appear always.

In Fig. 4, the shape of the leading mode in each one of the three cases studied is presented. The first case show minor changes in the mode, mostly on the radial component of the velocity v_r and on the center line, where the initial case exhibits the greatest amplitude. The strongest

	η [%]	NO [ppm]	NO_2 [ppm]	NO_x [ppm]
Initial	93.61	51.77	12.53	64.30
Case 1	92.33	47.82 (-8%)	11.85 (-5%)	59.60 (-7%)
Case 2	96.70	45.40 (-12%)	9.51 (-24%)	54.91 (-15%)
Case 3	91.74	44.26 (-15%)	17.60 (+40%)	61.92 (-4%)

Table 1: Summary of the mean efficiency of the flame and the production of NOx for the initial case and the three cases studied applying the flow control algorithm.

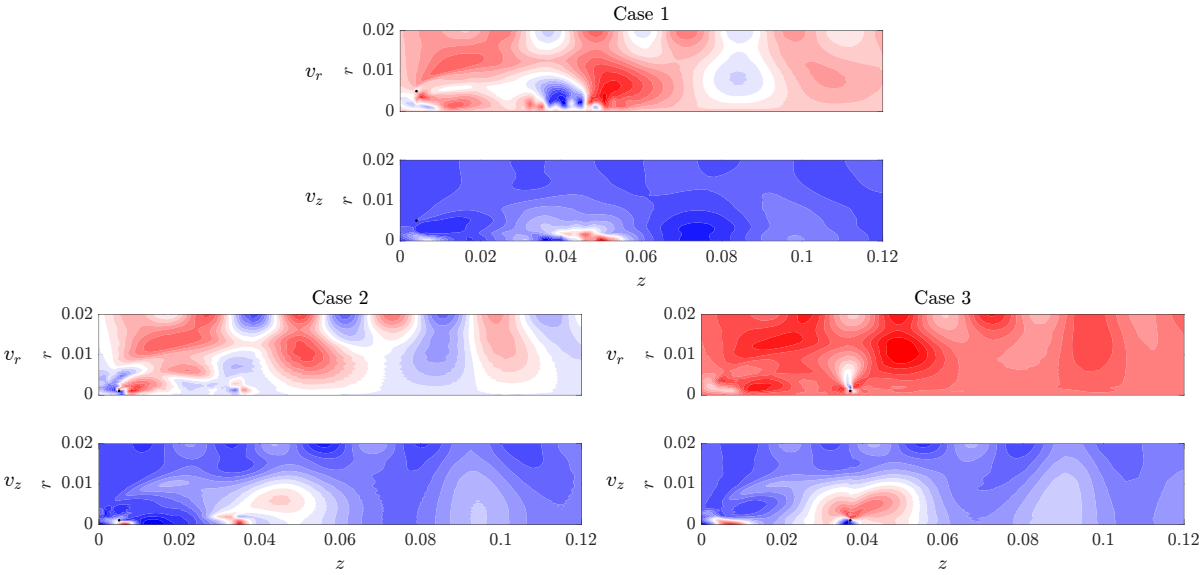

Figure 4: Real part of the leading mode for the velocity field in the three cases studied after applying the non-linear structural sensitivity algorithm, being v_r and v_z the radial and axial component, respectively. The mode has been normalized between values -1 and 1.

change in the shape of the mode appears in the second case, mostly on v_r, where the complexity of the mode increases considerably, suggesting a better mixing. Lastly in the third cases, the changes in the mode are mostly on the axial component of the velocity v_z, conducted by the appearance of a recirculation bubble downstream the cylinder inserted at $x = 0.001$; $z = 0.037$. Although this case has the lowest NO emissions, this significant change in the mode may be correlated with the highest NO_2 emissions. Further studies need to be carried out to understand what is the main mechanism triggering the reducction of emissions and rising the efficiency in the flame, but this is out of the scope of this paper.

5 CONCLUSIONS

The present work presents for the first time to the authors' knowledge a data driven algorithm for passive flow control in laminar flames. The algorithm locates the parts of the domain where the flow is more susceptible to changes. The method, as it is fully data-driven, is generalizable for different conditions of the flow and different geometries. The zones where the passive control is actuating provokes changes in the dynamics of the flow.

In particular, the algorithm has been applied to an axisymmetric, time varying, non-premixed

laminar co-flow flame. The flame has been studied with HODMD and it provides a periodic spectrum, due to the boundary condition of the fuel. The main mode locates in the center line.

The non-linear structural sensitivity provides three different parts of the domain where a little cylinder can be inserted for passive flow control. The results show a three point increase in the combustion efficiency and a reduction of 15% in the NO_x emissions, some of the most harmful pollutants. Applying HODMD to the three cases, it can be seen that the second case shows the strongest change in the mode, which appears on top of the oxidizer jet, in the main dynamics of the problem.

The results presented show great potential for the algorithm to be used in flow control applications and the design of components for pollutant reduction. However, the study should be extended to consider the influence that varying the size of the cylinder would have on the flow, as well as the inclusion of other variables in the gas mixture in the calculation of the non-linear structural sensitivity.

ACKNOWLEDGEMENTS

The authors acknowledge the grants PID2020-114173RB-I00, TED2021- 129774B-C21 and PLEC2022-009235 funded by MCIN/AEI/ 10.13039/501100011033 and by the European Union "NextGenerationEU"/PRTR, and S.L.C. acknowledges the support of Comunidad de Madrid through the call Research Grants for Young Investigators from Universidad Politécnica de Madrid. A.C. acknowledges the support of Universidad Politécnica de Madrid, under the program 'Programa Propio'. The MODELAIR and ENCODING project has received funding from the European Union's Horizon Europe research and innovation programme under the Marie Sklodowska-Curie grant agreement No. 101072559 and 101072779, respectively. The results of this publication reflect only the author(s) view and do not necessarily reflect those of the European Union. The European Union can not be held responsible for them. The authors gratefully acknowledge the Universidad Politécnica de Madrid (www.upm.es) for providing computing resources on Magerit Supercomputer.

REFERENCES

[1] Koumoutsakos, P. and Mezic I., 2006. "Control of Fluid Flow." Lecture Notes in Control and Information Sciences. https://doi.org/10.1007/978-3-540-36085-8

[2] Noack, B.R., Morzynski, M. and Tadmor G., 2011. "Reduced-Order Modelling for Flow Control." Springer Science and Business Media, New York, 528. https://doi.org/10.1007/978-3-7091-0758-4

[3] Cant, S., 2002. "High-performance computing in computational fluid dynamics: progress and challenges." Philos. Transact. A Math. Phys. Eng. Sci., 360(1795), 1211—1225. https://doi.org/10.1098/rsta.2002.0990

[4] Karagozian, A., 1999. "Control of mixing and reactive flow processes." 30th Fluid Dynamics Conference. https://doi.org/10.2514/6.1999-3572

[5] Beér, J.M. and Chigier, N.A., 1983. "Combustion Aerodynamics." Fuel and energy science series. https://doi.org/10.1017/S0022112072210990

[6] Karagozian, A.R., Wang, K.C., Le, A.-T. and Smith, O.I., 1996. "Transverse gas jet injection behind a rearward-facing step." J. Propul. Power, 12(6), 1129–1136. https://doi.org/10.2514/3.24153

[7] Giannetti, F. and Luchini, P., 2007. "Structural sensitivity of the first instability of the cylinder wake." J. Fluid Mech., 581, 167—197. https://doi.org/10.1017/S0022112007005654

[8] Varela, P., Suárez, P., Alcántara-Ávila, F., Miró, A., Rabault, J., Font, B., García-Cuevas, L.M., Lehmkuhl, O. and Vinuesa, R., 2022. "Deep Reinforcement Learning for Flow Control Exploits Different Physics for Increasing Reynolds Number Regimes." Actuators, 11, 359. https://doi.org/10.3390/act11120359

[9] Guastoni, L., Rabault, J., Schlatter, P., Azizpour, H. and Vinuesa R., 2023. "Deep reinforcement learning for turbulent drag reduction in channel flows." Eur. Phys. J. E, 46, 27. https://doi.org/10.1140/epje/s10189-023-00285-8

[10] Corrochano, A. and Le Clainche, S., 2022. "Structural sensitivity in nonlinear flows using direct solutions." Comput. Math. Appl., 128, 69–78. https://doi.org/10.1016/j.camwa.2022.10.006

[11] Le Clainche, S. and Vega, J.M., 2017. "Higher Order Dynamic Mode Decomposition." SIAM J. Appl. Dyn. Syst., 16(2), 882–925. https://doi.org/10.1137/15M1054924

[12] Schmid, P., 2010. "Dynamic mode decomposition of numerical and experimental data." J. Fluid Mech., 656, 5–28. https://doi.org/10.1137/15M1054924

[13] Amor, C., Corrochano, A., Foggi, G., Rosti, M.E. and Le Clainche, S., 2024. "Coherent structures in elastic turbulent planar jets." J. Phys.: Conf. Ser., 2753, 012020. https://dx.doi.org/10.1088/1742-6596/2753/1/012020

[14] Corrochano, A., D'Alessio, G., Parente, A. and Le Clainche, S., 2023. "Higher order dynamic mode decomposition to model reacting flows." Int. J. Mech. Sci., 249, 108219. https://doi.org/10.1016/j.ijmecsci.2023.108219

[15] Le Clainche, S., Han. Z. and Ferrer, E., 2019. "An alternative method to study crossflow instabilities based on high order dynamic mode decomposition" Phys. Fluids,31 (9). https://doi.org/10.1063/1.5110697

[16] Le Clainche, S., Rosti, M., and Brandt, L., 2022. "A data-driven model based on modal decomposition: application to the turbulent channel flow over an anisotropic porous wall", J. Fluid Mech., 939, A5. https://doi.org/10.1017/jfm.2022.159

[17] Vega, J.M. and Le Clainche, S., 2020. "Higher order dynamic mode decomposition and its applications." Elsevier. https://doi.org/10.1016/C2019-0-00038-6

[18] Hetherington, A., Corrochano, A., Abadía-Heredia, R., Lazpita, E., Muñoz, E., Díaz, P., Maiora, E., López-Martín, M. and Le Clainche, S., 2024. "ModelFLOWs-app: Data-driven post-processing and reduced order modelling tools." Comput. Phys. Commun., 301, 109217. https://doi.org/10.1016/j.cpc.2024.109217

[19] Smith, P.G., 1999. "GRI-Mech 3.0." http://www. me. berkley. edu/gri_mech/

[20] D'Alessio, G., Parente, A., Stagni, A. and Cuoci, A., 2020. "Adaptive chemistry via pre-partitioning of composition space and mechanism reduction." Combust. Flame, 211, 68–82. https://doi.org/10.1016/j.combustflame.2019.09.010

[21] D'Alessio, G., Cuoci, A., Aversano, G., Bracconi, M., Stagni, A. and Parente, A., 2020. "Impact of the partitioning method on multidimensional adaptive-chemistry simulations." Energies, 13(10), 2567. https://doi.org/10.3390/en13102567

[22] Parente, A. and Sutherland, J.S., 2013. "Principal component analysis of turbulent combustion data: Data pre-processing and manifold sensitivity." Combust. Flame, 160(2), 340–350. https://doi.org/10.1016/j.combustflame.2012.09.016